Disorder-Driven Transition from $s_\pm$ to s_{++} Superconducting Order Parameter in Proton Irradiated $Ba(Fe_{1-x}Rh_x)_2As_2$ Single Crystals

G. Ghigo,[1,2,*] D. Torsello,[1,2] G. A. Ummarino,[1,3] L. Gozzelino,[1,2] M. A. Tanatar,[4,5] R. Prozorov,[4,5] and P. C. Canfield[4,5]
[1]*Politecnico di Torino, Department of Applied Science and Technology, Torino 10129, Italy*
[2]*Istituto Nazionale di Fisica Nucleare, Sezione di Torino, Torino 10125, Italy*
[3]*National Research Nuclear University MEPhI (Moscow Engineering Physics Institute), Moskva 115409, Russia*
[4]*Ames Laboratory, US Department of Energy, Ames, Iowa 50011, USA*
[5]*Department of Physics & Astronomy, Iowa State University, Ames, Iowa 50011, USA*

(Received 1 June 2018; published 4 September 2018)

Microwave measurements of the London penetration depth and critical temperature T_c were used to show evidence of a disordered-driven transition from $s_\pm$ to s_{++} order parameter symmetry in optimally doped $Ba(Fe_{1-x}Rh_x)_2As_2$ single crystals, where disorder was induced by means of 3.5 MeV proton irradiation. Signatures of such a transition, as theoretically predicted [V. D. Efremov *et al.*, Phys. Rev. B **84**, 180512(R) (2011)], are found as a drop in the low-temperature values of the London penetration depth and a virtually disorder-independent superconducting T_c. We show how these experimental observations can be described by multiband Eliashberg calculations in which the effect of disorder is accounted for in a suitable way. To this aim, an effective two-band approach is adopted, allowing us to treat disorder in a range between the Born approximation and the unitary limit.

DOI: 10.1103/PhysRevLett.121.107001

Introduction.—Iron based superconductors (IBS) are nowadays among the most studied superconducting materials. They stimulated interest both due to their potential technological impact and their intriguing fundamental multiband and pairing properties. The leading candidate pairing state of most IBS, and, in particular, of the compounds based on doped $BaFe_2As_2$ (122-family), is the fully gapped $s_\pm$ phase [1,2]. This consists of an extended s-wave pairing with a sign reversal of the order parameter between different Fermi surface sheets and with interband coupling between hole and electron bands provided by antiferromagnetic spin fluctuations. Although this model is widely accepted, direct experimental confirmations are rare.

A promising approach to identify this phase makes use of disorder to induce a transition between the $s_\pm$ and s_{++} symmetries, therefore assigning the $s_\pm$ state to the pristine material [3,4]. This transition should occur because the gaps tend to converge with increasing disorder [4]: if the pristine state is characterized by the $s_\pm$ symmetry and the gaps converge to a finite value, it inevitably implies the closing and reopening of the smallest gap(s) and the realization of the s_{++} symmetry. It was suggested that this transition could leave specific hallmarks in the low temperature quasiparticle conductivity and London penetration depth, but they were observed experimentally only in the former [5]. The s_{++} state is characterized by the absence of sign reversal between different bands and has different properties from the $s_\pm$ state. In particular, the critical temperature of an s_{++} superconductor is expected to show a weaker disorder dependence.

In this Letter, we aim to observe and identify the hallmark of the $s_\pm$ to s_{++} transition driven by the proton-irradiation-induced disorder in the London penetration depth λ_L of $Ba(Fe_{1-x}Rh_x)_2As_2$ single crystals, by employing a microwave resonator technique. Ion irradiation is an efficient tool to introduce disorder into materials without contributing to charge doping or huge structural distortions. The choice of light projectiles at moderate energies such as 3.5-MeV protons ensures that only isotropically distributed pointlike defects and small cascades are produced in the system, provided that the thickness of the sample is smaller than the implantation depth of the ions. Then, we show how the $\lambda_L(T)$ experimental behavior and the $s_\pm$ to s_{++} transition can be described in a quantitative way by Eliashberg calculations where disorder is suitably accounted for. Thus the Letter is organized as follows: after a background about the electronic structure of the compound and the $s_\pm$ to s_{++} transition, the experimental and theoretical techniques are presented. Then, the results are discussed in light of the possible transition, and finally conclusions are drawn.

The $s_\pm$ to s_{++} transition.—The electronic structure of Ba-122 compounds can be approximately described by a three-band model. The nature of such bands depends on doping: two hole bands and one equivalent electron band for hole-doped compounds, as $Ba_{1-x}K_xFe_2As_2$, one hole band and two electron bands for electron-doped materials, as $Ba(Fe_{1-x}Co_x)_2As_2$. With this regard, there is a lack of literature about $Ba(Fe_{1-x}Rh_x)_2As_2$, but since Rh and Co are isoelectronic species and very similar experimental

behaviors were observed [6,7], it is reasonable to assume for both Rh- and Co-doped Ba-122 the same electronic structure.

Within the $s_\pm$ wave model, due to the antiferromagnetic spin fluctuation coupling, the gap of the electron band has opposite sign with respect to the gaps of the hole bands [2]. Recently, sign-reversal $s_\pm$ symmetry of the order parameter has been proved for $Ba_{1-x}Na_xFe_2As_2$ by phase-sensitive measurements [8], and it was even possible to induce it by disorder in the case of $BaFe_2(As_{1-x}P_x)_2$, which shows accidental gap nodes when in the pristine state [9]. This demonstrates that the topology of the superconducting gap can be controlled by disorder: a unique feature of the iron pnictides. Moreover, even much more complex situation can occur in the presence of an external field or superconducting currents, when coexistence of s_{++} and $s_\pm$ superconducting states in dirty multiband superconductors can be detected [10], but these peculiar conditions are not considered here.

Thus, a three-band $s_\pm$ model is the most appropriate to correctly describe the physical properties of these compounds. Recently, we have used such an approach to successfully explain the measured temperature dependence of the London penetration depth of $Ba_{1-x}K_xFe_2As_2$ crystals [11]. In another work, we have investigated the effects of irradiation-induced disorder on the properties of the same crystals [12]. Because of the fact that disorder was moderate, we could use the same three-band approach, treating disorder within the Born approximation: we were able to reproduce both the experimental T_c reduction and the $\lambda_L(T)$ behavior of the irradiated crystals, with the remarkable result of a change of sign of the smaller gap for the most disordered sample, but preserving the $s_\pm$ symmetry [12].

In this Letter, aiming at investigating the $s_\pm$ to s_{++} transition, we want to analyze the case of $Ba(Fe_{1-x}Rh_x)_2As_2$ with a much higher degree of disorder, when the Born approximation is expected to lose its validity. The problem emerges that in such a framework the three-band calculations become tricky and the parameter space enlarges too much to allow drawing reasonable conclusions. For these reasons, we implemented a T-matrix approach within an effective two-band model, allowing us to treat disorder in a range from the Born approximation to the unitary limit. Accordingly, we consider both *interband* and *intraband* scattering, but it is intended that intraband terms have no direct physical meaning, representing a combination of interband terms of a more realistic three-band model. In fact, it can be said that in these systems the interband coupling is predominant [13].

On this premise, we look for the experimental signatures of a disordered-induced $s_\pm$ to s_{++} transition, i.e., a transition to a state where the sign of the two (or more) gaps is preserved. The signature we are focusing on is a drop in the low-temperature value of λ_L, as qualitatively predicted, but not yet observed [4,5]. Then, we show how this experimental behavior can be described by a two-band Eliashberg model.

Experimental techniques.—Optimally doped single crystals of $Ba(Fe_{1-x}Rh_x)_2As_2$, with $x = 0.068$ and critical temperature $T_{c0} = 23.5$ K, were grown out of self-flux using conventional high-temperature solution growth techniques [14–16]. The investigated samples were cleaved to have thickness, along the c axis, smaller than the implantation depth of 3.5 MeV protons in the material. The characterization of their superconducting properties was carried out by means of a microwave resonator technique that has already been applied to other IBS crystals [11,12,17]. It allows obtaining the absolute value of the London penetration depth and the surface impedance as a function of temperature by measuring the modifications induced to the resonance of an $YBa_2Cu_3O_{7-x}$ coplanar waveguide resonator by coupling the sample to it [18]. Since the technique is nondestructive, it is suitable for measurements on the pristine crystals and after each irradiation session, in order to observe the evolution of the superconducting properties with increasing disorder, avoiding sample-to-sample variability.

Proton irradiation was performed at the CN facility of the LNL laboratories of the Italian National Institute for Nuclear Physics (INFN). The samples were irradiated with 3.5 MeV protons in multiple sessions, up to a total fluence of 2.08×10^{17} cm^{-2}. Further details are reported in Ref. [18]. The irradiation process was addressed by Monte Carlo simulations performed with the PHITS [29] and SRIM [30] codes in order to replicate the experimental conditions and estimate the irradiation effects on the samples. To this aim, the displacement per atom (dpa) profile as a function of depth inside the material was estimated within the Kinchin-Pease approach [18]. This allows us to obtain the position of the implantation peak in the material, that would be at about 67 μm, and in turn to keep the thickness of the samples well below this value to avoid ion implantation. Moreover, the amount of introduced disorder in a particular crystal is estimated as the dpa averaged over its thickness.

Figure 1 shows the critical temperature T_c of an irradiated crystal normalized to its pristine value and the width of the superconducting transition, as a function of disorder expressed by the irradiation-induced displacement per atom. In the lower panel of Fig. 1, experimental low-temperature values of the London penetration depth are reported. T_c and $\lambda_L(0)$ show a clear change of behavior at a given value of disorder, highlighted in the figure by a change in the background color, while the unaltered increase of the transition width testifies that disorder continuously increases. In particular, as stated in the Introduction, the clear drop of $\lambda_L(0)$ can be considered to be a sign of the transition from the $s_\pm$ to the s_{++} state. Basing this hypothesis on the experimental results, we

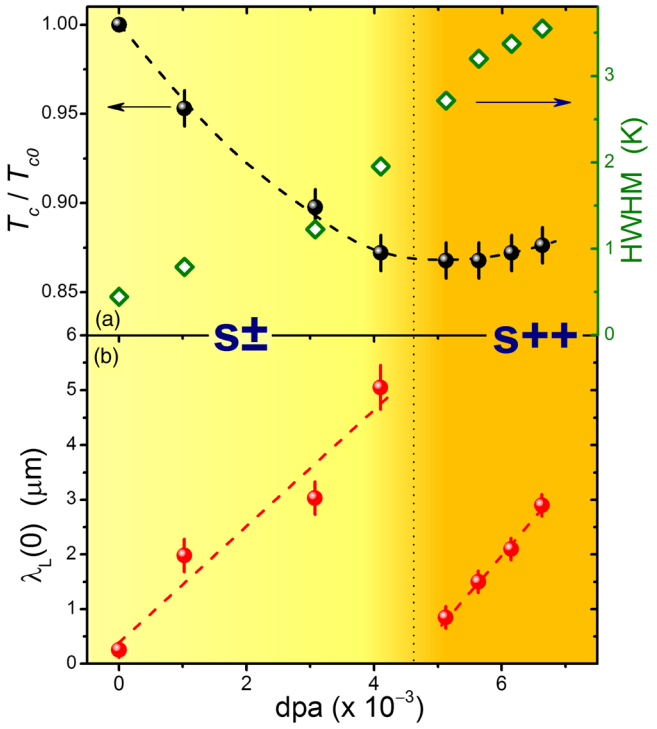

FIG. 1. (a) Critical temperature of the irradiated crystal normalized to its value for the pristine crystal, as a function of the irradiation-induced disorder, expressed by the average displacement per atom. The critical temperature considered here is the temperature of $\lambda(T)$ divergence. The width of the superconducting transition is shown as the half-width-half-maximum value of the derivative of $1/Q$ raw data (right scale). (b) Low-temperature values of the London penetration depth. Different background colors are used to qualitatively distinguish between the $s_{\pm}$ and s_{++} phases, discussed throughout this Letter. The transition between them is identified in the $\lambda_L(0)$ drop, as discussed in the text (dashed lines are guides to the eye).

propose in the following a model that could validate it within realistic assumptions. For the sake of completeness, we should say that Schilling *et al.* [5], tracing the $s_{\pm}$ to s_{++} transition in the related material $Ba(Fe_{1-x}Co_x)_2As_2$ by observing the behavior of the optical conductivity, did not discern the discontinuity of $\lambda_L(0)$. This is not in contrast with our results since the experimental conditions were very different as for the compound, the morphology (thin film in Ref. [5]) and the particle (200-keV protons in Ref. [5]).

Figure 1 also shows that T_c starts to slightly recover, at the higher disorder values. This behavior can be explained by two opposite scenarios. A T_c enhancement can be attributed to the competition between superconductivity and a secondary order (spin density wave) that is suppressed more rapidly by disorder than superconductivity itself [31]. Conversely, the induction of a local magnetic phase could stabilize the superconductivity, even leading to a slight enhancement of the superconducting order parameter [32] (indeed, we observed a magnetic phase in proton-irradiated crystals [16]). In both cases, it results that this feeble effect can only emerge in the s_{++} state, where the pair-breaking effect of disorder is much weaker than in the $s_{\pm}$ state.

The model.—To calculate the critical temperature and the penetration depth within the $s_{\pm}$ wave by the two-band Eliashberg equations [33], one has to solve four coupled equations for the gaps $\Delta_i(i\omega_n)$ and renormalization functions $Z_i(i\omega_n)$, where i is a band index and ω_n are the Matsubara frequencies. The imaginary-axis equations [33–35] read

$$\omega_n Z_i(i\omega_n) = \omega_n + \pi T \sum_{m,j} \Lambda^Z_{ij}(i\omega_n, i\omega_m) N^Z_j(i\omega_m) + \sum_j \Gamma^N_{ij} N^Z_j(i\omega_n), \quad (1)$$

$$Z_i(i\omega_n)\Delta_i(i\omega_n) = \pi T \sum_{m,j} [\Lambda^{\Delta}_{ij}(i\omega_n, i\omega_m) - \mu^*_{ij}(\omega_c)] \times \Theta(\omega_c - |\omega_m|) N^{\Delta}_j(i\omega_m) + \sum_j \Gamma^N_{ij} N^{\Delta}_j(i\omega_n), \quad (2)$$

where Γ^N_{ij} are the scattering rates from nonmagnetic impurities (the diagonal components Γ^N_{ii} do not affect the superconductive properties):

$$\Gamma^N_{12(21)} = \frac{\Gamma_{1(2)}(1-\sigma)}{\sigma(1-\sigma)\eta[N_1(0)+N_2(0)]^2/N_1(0)N_2(0) + (\sigma\eta - 1)^2},$$

where $\sigma = \pi^2 N_1(0) N_2(0) u^2 / [1 + \pi^2 N_1(0) N_2(0) u^2]$ and $\Gamma_{1(2)} = n_{\mathrm{imp}} \pi N_{2(1)}(0) u^2 (1-\sigma)$ are the generalized cross section and normal state scattering rate parameters, respectively, and n_{imp} is the impurity concentration. The parameter η controls the ratio of intraband and interband scattering as $v^2 = u^2 \eta$, where v and u are the intraband and interband parts of the impurity potential, respectively [34,36]. When $\sigma \to 0$, disorder is treated within the Born limit (weak scattering), while for $\sigma \to 1$ the unitary limit is achieved (strong scattering). Thus, disorder is controlled by three parameters, namely, σ, η, and Γ_1, since $\Gamma_2 = \Gamma_1 [N_1(0)/N_2(0)]$. As for the ratio of the normal densities of states at the Fermi level, $N_1(0)/N_2(0)$, we assume the value obtainable for the similar electron-doped compound $Ba(Fe_{1-x}Co_x)_2As_2$ by summing the contributions of the electronic bands of the three-band model [18]. The other parameters explicitly or implicitly present in Eqs. (1) and (2), as the components of the electron-boson coupling-constant matrix λ_{ij}, the input values and the approximations are described in detail in Ref. [18].

Within a multiband model and disregarding the anisotropy, the penetration depth of the magnetic field, λ_L, in the London limit [37], is expressed as

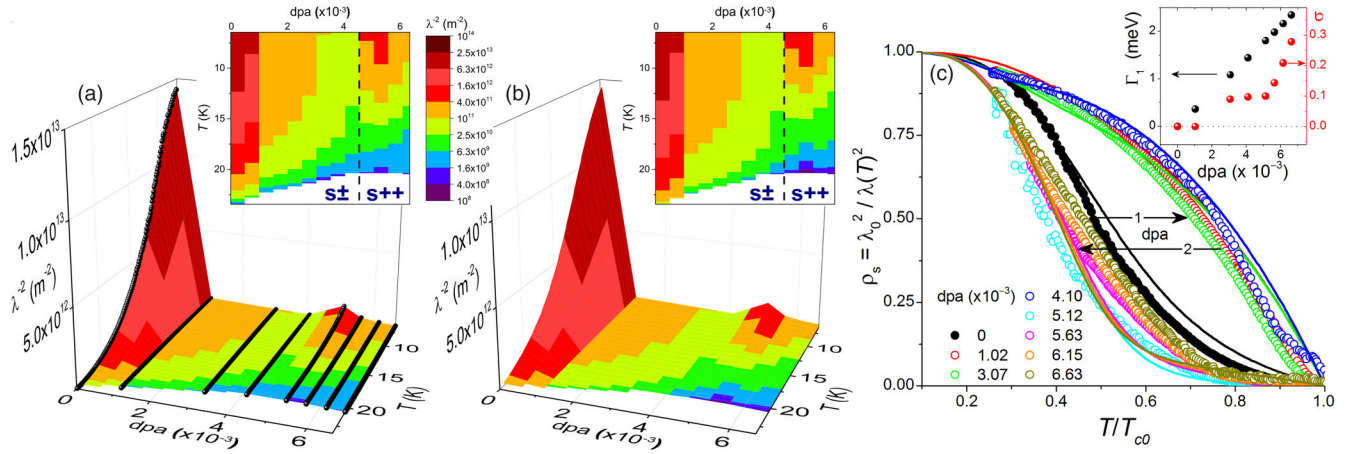

FIG. 2. λ_L^{-2} as a function of temperature and disorder (dpa): (a) Experimental and (b) calculated surface plots. In (a) the experimental curves are superimposed as symbols. The insets show the corresponding two-dimensional color plots, where the $s_\pm$ to s_{++} transition is marked by a dashed line. All the graphs refer to the same color scale. The superfluid density is reported as a function of the reduced temperature in (c), where the experimental data (symbols) are compared to calculations (lines). The shape clearly changes after first irradiation doses (arrow #1) and again after the $s_\pm$ to s_{++} transition (arrow #2). Calculated curves correctly describe this behavior, but fail to exactly reproduce the experimental results, mainly because of the compulsory choice to treat disorder within an effective two-gap model. The inset shows the values of the parameters Γ_1 and σ as a function of dpa.

$$\lambda_L^{-2}(T) = \left(\frac{\omega_p}{c}\right)^2 \sum_{i=1}^{3} \left(\frac{\omega_{p,i}}{\omega_p}\right)^2 \pi T \times \sum_{n=-\infty}^{+\infty} \frac{\Delta_i^2(\omega_n) Z_i^2(\omega_n)}{[\omega_n^2 Z_i^2(\omega_n) + \Delta_i^2(\omega_n) Z_i^2(\omega_n)]^{3/2}}, \quad (3)$$

where c is the speed of light, $Z_i(\omega_n)$ and $\Delta_i(\omega_n)$ are the solutions of the Eliashberg equations and $\omega_{p,i}$ is the plasma frequency associated to band i. Then, the superfluid density can be computed as $\rho_s(T) = \lambda_L^2(0)/\lambda_L^2(T)$. The values of the plasma frequencies $\omega_{p,i}$ for each band are unknown, but since the weights in Eq. (3) are normalized to unity, $(\omega_{p,1}/\omega_p)^2 + (\omega_{p,2}/\omega_p)^2 = 1$, a single free parameter can be considered for fitting the experimental data, $w_1 = (\omega_{p,1}/\omega_p)^2$.

We reproduced the experimental T_c and $\rho_s(T)$ in the nondisordered case (unirradiated crystal) with $\lambda_{11} = 1.0$, $\lambda_{22} = 2.65$, and $\lambda_{12} = -0.17$, for a total coupling $\lambda_{\text{tot}} = \{[N_1(0)(\lambda_{11}+\lambda_{12}) + N_2(0)(\lambda_{21}+\lambda_{22})]/[N_1(0)+N_2(0)]\} = 1.74$, and with $w_1 = 0.98$. In this case, the Eliashberg equations at $T = 0.5$ K gave the low-temperature values of the gaps, $\Delta_1 = -2.64$ and $\Delta_2 = 5.71$ meV, which are actually obtained by the analytical continuation to the real axis of the imaginary-axis solutions of Eqs. (1) and (2), by using the technique of the Padé approximants.

To describe the effects of disorder we can operate on Γ_{ij}^N, which include the three free parameters Γ_1, σ, and η, proportional to structural disorder in an *a priori* unknown way.

Discussion.—The model described above is now used to reproduce the experimental results, i.e., T_c and $\rho_s(T)$ of disordered samples, assuming reasonable values for the parameters: we keep $\eta = 1$, as in Ref. [5], Γ_1 linearly increasing with the irradiation dose (from 0 to 2.35 meV for the most irradiated crystal), and σ increasing from 0 (Born limit, unirradiated crystal) to 0.278. The weight w_1 is then adjusted to better fit the data. The values of the parameters allowing us to better reproduce the experimental results are reported in the inset of Fig. 2(c) and, as a table, in Ref. [18]. In Figs. 2(a)–2(b) the experimental values of $\lambda_L^{-2}(T)$ as a function of temperature and disorder are compared to calculations based on Eq. (3), showing a remarkable matching. The $s_\pm$ to s_{++} transition is identified at a dpa value of about 0.0046. The superfluid density is reported as a function of the reduced temperature in Fig. 2(c), where the experimental data (symbols) are compared to calculations (lines). The shape clearly changes after first irradiation doses and again after the $s_\pm$ to s_{++} transition. The calculated curves correctly describe the general behavior, but fail to reproduce the experimental data exactly, mainly because of the approximation of considering two effective gaps instead of at least three (more realistic model), imposed by the need to suitably describe the effects of disorder. This choice, together with the assumptions we made to limit the parameter space, impose severe constraints to the results of the calculations. Finally, Fig. 3 shows the calculated gaps, resulting from such parameters. On the left, the energy gaps obtained by the solution of the imaginary-axis Eliashberg equations, for the same crystal before and after each irradiation, are given. On the right, the low-temperature values of the gaps from the real-axis solutions of the Eliashberg equations, obtained by the Padé approximants, are reported as a function of disorder. The transition from a sign-reversal to a sign-preserving symmetry of the order parameter is shown at the same

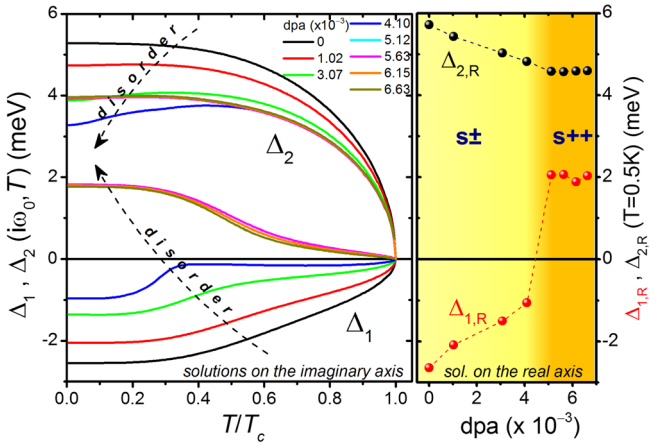

FIG. 3. Left: temperature dependence of the energy gaps obtained by the solution of the imaginary-axis Eliashberg equations, for the unirradiated crystal (black lines) and for the same crystal after each irradiation (color lines). As the irradiation-induced disorder increases, Δ_1 and Δ_2 get closer, with Δ_1 changing sign for the most irradiated samples. Right: low-temperature values of the gaps from the real-axis solutions of the Eliashberg equations, obtained by the Padé approximants, as a function of disorder, expressed here in terms of irradiation-induced displacement per atom (dpa). The transition from the $s_\pm$ to s_{++} state is highlighted by the change in the background colors.

disorder level as in Figs. 1 and 2. In the s_{++} state, the difference between Δ_1 and Δ_2 does not continue to decrease, which is consistent with the T_c behavior discussed above.

Conclusions.—We have shown, by means of a microwave technique, the experimental evidence of a disordered-induced $s_\pm$ to s_{++} transition in $Ba(Fe_{1-x}Rh_x)_2As_2$ single crystals, in the form of a clear drop in the low-temperature values of the London penetration depth, as already predicted in literature but not yet observed. Disorder was induced by 3.5-MeV proton irradiation, up to 6.63×10^{-3} displacements per atom. The transition was validated through a two-band Eliashberg model, where disorder is considered in a variable range between the Born approximation and the unitary limit. Self-consistent calculations with realistic parameter values reproduced the experimental critical temperature and superfluid density, with the $s_\pm$ to s_{++} transition at the expected disorder level. The agreement is only semiquantitative, since at least three bands should be considered to correctly describe the physics of the compound, but this was made impractical by the need to correctly account for a high level of disorder.

In summary, our approach is an effective and general way to determine whether a material is characterized by the $s_\pm$ symmetry, through its evolution with disorder. Hopefully, these findings will stimulate the development of further experiments aimed to shed more light onto the underlying coupling mechanisms.

The authors thank P. Carretta, D. V. Efremov, and P. J. Hirschfeld for fruitful discussions, and the INFN-LNL staff for help with the irradiation experiments. Work done at Ames Lab (M. A. T., R. P., P. C. C.) was supported by the U.S. Department of Energy, Office of Basic Energy Science, Division of Materials Sciences and Engineering. Ames Laboratory is operated for the U.S. Department of Energy by Iowa State University under Contract No. DE-AC02-07CH11358. G. A. U. acknowledges the support from the MEPhI Academic Excellence Project (Contract No. 02.a03.21.0005).

*Corresponding author.
gianluca.ghigo@polito.it

[1] A. V. Chubukov, D. V. Efremov, and I. Eremin, Phys. Rev. B **78**, 134512 (2008).
[2] I. I. Mazin, D. J. Singh, M. D. Johannes, and M. H. Du, Phys. Rev. Lett. **101**, 057003 (2008).
[3] Y. Wang, A. Kreisel, P. J. Hirschfeld, and V. Mishra, Phys. Rev. B **87**, 094504 (2013).
[4] D. V. Efremov, M. M. Korshunov, O. V. Dolgov, A. A. Golubov, and P. J. Hirschfeld, Phys. Rev. B **84**, 180512(R) (2011).
[5] M. B. Schilling, A. Baumgartner, B. Gorshunov, E. S. Zhukova, V. A. Dravin, K. V. Mitsen, D. V. Efremov, O. V. Dolgov, K. Iida, M. Dressel, and S. Zapf, Phys. Rev. B **93**, 174515 (2016).
[6] M. A. Tanatar, N. Ni, A. Thaler, S. L. Bud'ko, P. C. Canfield, and R. Prozorov, Phys. Rev. B **84**, 014519 (2011).
[7] H. Kim, M. A. Tanatar, C. Martin, E. C. Blomberg, N. Ni, S. L. Bud'ko, P. C. Canfield, and R. Prozorov, J. Phys. Condens. Matter **30**, 225602 (2018).
[8] A. A. Kalenyuk, A. Pagliero, E. A. Borodianskyi, A. A. Kordyuk, and V. M. Krasnov, Phys. Rev. Lett. **120**, 067001 (2018).
[9] Y. Mizukami, M. Konczykowski, Y. Kawamoto, S. Kurata, S. Kasahara, K. Hashimoto, V. Mishra, A. Kreisel, Y. Wang, P. J. Hirschfeld, Y. Matsuda, and T. Shibauchi, Nat. Commun. **5**, 5657 (2014).
[10] J. Garaud, A. Corticelli, M. Silaev, and E. Babaev, Phys. Rev. B **97**, 054520 (2018).
[11] G. Ghigo, G. A. Ummarino, L. Gozzelino, and T. Tamegai, Phys. Rev. B **96**, 014501 (2017).
[12] G. Ghigo, G. A. Ummarino, L. Gozzelino, R. Gerbaldo, F. Laviano, D. Torsello, and T. Tamegai, Sci. Rep. **7**, 13029 (2017).
[13] L. Boeri, M. Calandra, I. I. Mazin, O. V. Dolgov, and F. Mauri, Phys. Rev. B **82**, 020506 (2010).
[14] N. Ni, M. E. Tillman, J.-Q. Yan, A. Kracher, S. T. Hannahs, S. L. Bud'ko, and P. C. Canfield, Phys. Rev. B **78**, 214515 (2008).
[15] N. Ni, A. Thaler, A. Kracher, J. Q. Yan, S. L. Bud'ko, and P. C. Canfield, Phys. Rev. B **80**, 024511 (2009).
[16] M. Moroni, L. Gozzelino, G. Ghigo, M. A. Tanatar, R. Prozorov, P. C. Canfield, and P. Carretta, Phys. Rev. B **96**, 094523 (2017).
[17] G. Ghigo, D. Torsello, R. Gerbaldo, L. Gozzelino, F. Laviano, and T. Tamegai, Supercond. Sci. Technol. **31**, 034006 (2018).

[18] See Supplemental Material at http://link.aps.org/supplemental/10.1103/PhysRevLett.121.107001 for further details on the experimental techniques, on the irradiation process, and on the model calculations, which also includes Refs. [19–28].
[19] G. Ghigo, F. Laviano, R. Gerbaldo, and L. Gozzelino, Supercond. Sci. Technol. **25**, 115007 (2012).
[20] G. Ghigo, R. Gerbaldo, L. Gozzelino, F. Laviano, and T. Tamegai, IEEE Trans. Appl. Supercond. **26**, 1 (2016).
[21] W. N. Hardy, D. A. Bonn, D. C. Morgan, R. Liang, and K. Zhang, Phys. Rev. Lett. **70**, 3999 (1993).
[22] R. Prozorov, R. W. Giannetta, A. Carrington, and F. M. Araujo-Moreira, Phys. Rev. B **62**, 115 (2000).
[23] I. Vendik, Supercond. Sci. Technol. **13**, 974 (2000).
[24] G. A. Ummarino, M. Tortello, D. Daghero, and R. S. Gonnelli, Phys. Rev. B **80**, 172503 (2009).
[25] D. Isonov, J. Park, P. Bourges, D. Sun, Y. Sidis, A. Schneidewind, K. Hradil, D. Haug, C. Lin, B. Keimer, and V. Hinkov, Nat. Phys. **6**, 178 (2010).
[26] J. Paglione and R. Greene, Nat. Phys. **6**, 645 (2010).
[27] P. J. Hirschfeld, M. M. Korshunov, and I. I. Mazin, Rep. Prog. Phys. **74**, 124508 (2011).
[28] I. Mazin and J. Schmalian, Physica (Amsterdam) **469C**, 614 (2009).
[29] T. Sato, K. Niita, N. Matsuda, S. Hashimoto, Y. Iwamoto, S. Noda, T. Ogawa, H. Iwase, H. Nakashima, T. Fukahori, K. Okumura, T. Kai, S. Chiba, T. Furuta, and L. Sihver, J. Nucl. Sci. Technol. **50**, 913 (2013).
[30] J. F. Ziegler, M. Ziegler, and J. Biersack, Nucl. Instrum. Methods Phys. Res., Sect. B **268**, 1818 (2010).
[31] S. Teknowijoyo, K. Cho, M. A. Tanatar, J. Gonzales, A. E. Böhmer, O. Cavani, V. Mishra, P. J. Hirschfeld, S. L. Bud'ko, P. C. Canfield, and R. Prozorov, Phys. Rev. B **94**, 064521 (2016).
[32] M. N. Gastiasoro, F. Bernardini, and B. M. Andersen, Phys. Rev. Lett. **117**, 257002 (2016).
[33] G. M. Eliashberg, JETP **11**, 696 (1960).
[34] M. M. Korshunov, Y. N. Togushova, and O. V. Dolgov, Phys. Usp. **59**, 1211 (2016).
[35] G. A. Ummarino, Phys. Rev. B **83**, 092508 (2011).
[36] V. A. Shestakov, M. M. Korshunov, Y. N. Togushova, D. V. Efremov, and O. V. Dolgov, Supercond. Sci. Technol. **31**, 034001 (2018).
[37] A. A. Golubov, A. Brinkman, O. V. Dolgov, J. Kortus, and O. Jepsen, Phys. Rev. B **66**, 054524 (2002).